TECHNICAL NOTE:

SATELLITE PSYCHROMETRIC FORMULATION OF THE OPERATIONAL SIMPLIFIED SURFACE ENERGY BALANCE (SSEBOP) MODEL FOR QUANTIFYING AND MAPPING EVAPOTRANSPIRATION

G. B. Senay

ABSTRACT. *Remote sensing-based evapotranspiration (ET) can be derived using various methods, from soil moisture accounting to vegetation-index based approaches to simple and complex surface energy balance techniques. Due to the complexity of fully representing and parameterizing ET sub-processes, different models tend to diverge in their estimations. However, most models appear to provide reasonable estimations that can meet user requirements for seasonal water use estimation and drought monitoring. One such model is the Operational Simplified Surface Energy Balance (SSEBop). This study presents a formulation of the SSEBop model using the psychrometric principle for vapor pressure/relative humidity measurements where the "dry-bulb" and "wet-bulb" equivalent readings can be obtained from satellite-based land surface temperature estimates. The difference in temperature between the dry (desired location) and wet limit (reference value) is directly correlated to the soil-vegetation composite moisture status (surface humidity) and thus producing a fractional value (0-1) to scale the reference ET. The reference ET is independently calculated using available weather data through the standardized Penman-Monteith equation. Satellite Psychrometric Approach (SPA) explains the SSEBop model more effectively than the energy balance principle because SSEBop does not solve all terms of the surface energy balance such as sensible and ground-heat fluxes. The SPA explanation demonstrates the psychrometric constant for the air can be readily adapted to a comparable constant for the surface, thus allowing the creation of a "surface" psychrometric constant that is unique to a location and day-of-year. This new surface psychrometric constant simplifies the calculation and explanation of satellite-based ET for several applications in agriculture and hydrology. The SPA formulation of SSEBop was found to be an enhancement of the ET equation formulated in 1977 by pioneering researchers. With only two key parameters, improved model results can be obtained using a one-time calibration for any bias correction. The model can be set up quickly for routine monitoring and assessment of ET at landscape scales and beyond.*

Keywords. *Dry-bulb, ET fraction, ET modeling, Remote sensing, Satellite psychrometry, Wet-bulb.*

The use of remote sensing data in hydrologic modeling has allowed the formulation of several approaches to estimate spatially explicit evapotranspiration (ET), which is a key hydrologic variable in the cycling of moisture between the land and atmosphere along with maintaining and providing a mechanism for cooling the land surface.

Although several existing models use satellite data for estimating ET, their complexity varies depending on the intended purpose and handling of ET sub-processes (e.g., Jackson et al., 1977, 1981; Moran et al., 1996; Anderson et al., 1997; Bastiaanssen et al., 1998; Kustas and Norman, 2000; Roerink et al., 2000; Su, 2002; Nagler et al., 2005; Fisher et al., 2005; Allen et al., 2007; Carlson, 2007; Glenn et al., 2007; Mu et al., 2011, Senay et al., 2007, 2013). Generally, most ET models tend to agree in capturing the overall spatial variability (e.g., Singh and Senay, 2015) that is a result of using similar model forcings derived from satellite data. The major differences among models appear to be in bias errors that could be a result of differences in model parameterization. The Operational Simplified Surface Energy

Submitted for review in September 2017 as manuscript number NRES 12614; approved for publication as a Technical Note by the Natural Resources & Environmental Systems Community of ASABE in February 2018.

Mention of company or trade names is for description only and does not imply endorsement by the USGS.

The author is **Gabriel B. Senay**, Research Physical Scientist, U.S. Geological Survey Earth Resources Observation and Science (EROS) Center/North Central Climate Science Center, NREL 1499, Colorado State University, Fort Collins, CO 80528; phone: 605-594-2758; e-mail: senay@usgs.gov.

Balance (SSEBop) is one of the simplest surface energy balance models for large-scale ET estimation as it directly solves for latent heat flux without the need to solve for the other components of the surface energy balance equation such as net radiation, sensible heat, and ground heat fluxes.

Because it does not solve the full surface energy balance components, the designation of SSEBop as a surface energy balance model has been met with some criticism. The main objective of this study is to demonstrate the application of psychrometric principles for ET mapping through the reformulation of the SSEBop ET model. Considering the presence of empirical parameters in all "full" energy balance models (Penman, 1948) and the philosophical statement of Penman (1948) "while mathematicians and physicists look for facts to fit the model, the practical engineer looks for a model to fit the facts", the proposed Satellite Psychrometric Approach (SPA) can be useful for understanding and explaining the physical basis of the SSEBop model using a more established principle of psychrometry and encourage users to adapt and experiment with the model to estimate ET in diverse hydro-climatic systems.

PSYCHROMETRY

By definition, psychrometry is a field of study that deals with the determination of the physical and thermodynamic properties of gas-vapor mixtures. The term derives from the Greek word *psuchron* meaning "cold" and *metron* for "means of measurement" (Liddell, 1940). It can simply be re-stated as the technique of measuring the water vapor content of air (relative humidity).

The use of psychrometry in micrometeorology has a long history dating back to the late 1800s (e.g., Ferrel, 1886). Lourence and Pruitt (1969) identified vertical profile measurements of air temperature and humidity over vegetated surfaces as the two vital parameters in micrometeorological studies.

A psychrometer for relative humidity measurement consists of two identical thermometers with one bulb kept wet (wet-bulb) while the other measures the ambient air temperature (dry-bulb). The wet-bulb thermometer registers a lower temperature as a result of the cooling effect of evaporation. The difference between the dry- and wet-bulb readings along with a psychrometric constant can be used to determine the relative humidity and actual vapor pressure of the air (Allen et al., 1998). The larger the difference between the dry-bulb and wet-bulb, the drier the air and the lower the relative humidity; similarly, the lower the difference, the higher the relative humidity, i.e., moist air.

One of the earliest linkages between psychrometry and evaporation was reported in the formulation of the Bowen ratio energy budget equation for estimating energy and vapor fluxes (Bowen et al., 1926; Fuchs and Tanner, 1970). The Bowen ratio assumes the diffusion coefficient for eddies of sensible and latent heat fluxes are equal, thus the ratio between the two fluxes is 1.0. Because of this unity, the Bowen ratio can be expressed as the ratio between air temperature and vapor pressure differences that are measured on two levels between the surface and air layer using the proportionality psychrometric constant. Penman (1955) developed the derivation of the theoretical basis for the formulation of the psychrometric constant as a function of the atmospheric pressure. Psychrometric measurements are taken when the rate of change of sensible heat is in dynamic equilibrium with the rate of change of latent heat at the wet-bulb. At the wet-bulb, flowing air removes heat through evaporative cooling, causing the temperature to drop. But this process creates a differential temperature with the surrounding air where heat will flow from the surrounding air (higher temperature) to the wet-bulb (lower temperature), countering the cooling effect. Thus, further cooling of the wet-bulb stops when it is in equilibrium with the heat gained from the surrounding air. Therefore, the wet-bulb temperature is the temperature of a surface that can be achieved through evaporative cooling under an equilibrium heat exchange condition.

The application of thermocouple psychrometry for soil water potential estimation has been documented by various researchers (e.g., Rawlins, 1966; Campbell, 1979) and plant transpiration by Slatyer and Bierhuizen (1964) through the use of a differential psychrometry setup. From differential psychrometry measurements, transpiration can be determined when relative humidity is multiplied by the density of water vapor in saturated air at the dry-bulb to get a water vapor concentration in mg/m^3. Thus, with knowledge of airflow through a test chamber, transpiration can be quantified as a product of air flow rate and vapor concentration (Slatyer and Bierhuizen, 1964).

METHODS: TECHNICAL DEVELOPMENT

SATELLITE PSYCHROMETRIC APPROACH (SPA) FORMULATION

The SPA formulation of SSEBop (eq. 1) requires the use of satellite-based surface temperature instead of air temperature, and the reformulation of the standard psychrometric constant shown in equation 2 to estimate the ET fraction, which will be used to scale the maximum ET derived from weather datasets.

$$ETf = 1 - \gamma^s \left(Ts - Tc \right) \quad (1)$$

where *ETf* is ET fraction, nominally varying between 0 and 1; γ^S is denoted as a "surface psychrometric" constant (SPC) based on the aerodynamic properties of a dry-bare surface (section 2.2) (K^{-1}); *Ts* is satellite-derived land surface temperature (LST, K); and *Tc* is the cold/wet limit surface temperature (K) derived from air temperature (Senay et al., 2013, 2016, 2017). The constant 1 represents the value of ET fraction during maximum ET, i.e., *Ts* = *Tc*.

Standard psychrometry uses measurements of the dry-bulb and wet-bulb thermometers to measure the ambient temperature of the air (dry-bulb) and the air that is cooled by the evaporation of water (wet-bulb). Thus, actual vapor pressure calculation can be formulated as shown in equation 2 (Allen et al., 1998).

$$ea = es - \gamma \left(Td - Tw \right) \quad (2)$$

where *ea* is actual vapor pressure (kPa); *es* is the saturation vapor pressure at temperature of *Tw* (kPa); *Tw* is the air temperature as measured by the wet-bulb thermometer (K); *Td*

is the air temperature measured by the dry-bulb thermometer (K); and γ is the psychrometric constant (kP.°C^{-1}).

If we divide both sides of equation 2 by *es*, the ratio of *ea* to *es* gives the relative humidity in fraction (eq. 3), which is a measure of the dryness of the air as the *ETf* in equation 1 gives the dryness of the surface (soil-vegetation composite).

$$RH = \frac{ea}{es} = 1 - \frac{\gamma(Td - Tw)}{es} \quad (3)$$

where RH is relative humidity in fraction (0-1).

In SPA, LST as measured by satellite sensors is used to estimate both the equivalent dry-bulb (*Ts*) at any pixel and the wet-bulb (*Tc*) surface reference temperatures. Thus, the difference between the measured satellite *Ts* and reference *Tc* is used to determine the ET fraction using the equivalent of the standard psychrometric constant, which is now denoted as surface psychrometric constant (SPC or γ^S) in equation 1.

Equation 2 dictates that when *Td* is close to *Tw*, RH is close to 100%, providing a measure for the state of the air as high humidity. A comparable look at equation 1 for ET fraction in SPA shows that when *Ts* is close to *Tc*, relative wetness of a surface is maximum or close to 1, implying the only limiting factor is the atmospheric demand, as represented by a scaled-up maximum reference ET.

A closer examination of equation 1 reveals that it is comparable to the "evapotranspiration equation" formulated by Jackson et al. (1977) as shown in equation 4. Particularly, dividing both sides of the equation by net radiation (*Rn*) will make the comparison on the basis of ET fraction. Equation 4 was developed to predict crop water use over large areas using remotely sensed parameters. Jackson et al. (1977) simplified the energy balance and aerodynamic calculations by developing an empirical "B" parameter to take into account the impact of aerodynamic forces and by ignoring the ground heat flux in the conservation of energy for a daily estimate.

$$ET = Rn - B(Tsc - Tac) \quad (4)$$

where *ET* is daily actual ET (cm); *Rn* is daily net radiation in depth units (cm); *B* is a "composite constant", a statistical parameter determined for each location from observed data (cm.K^{-1}); *Tsc* is canopy temperature (K); and *Tac* is air temperature (K) measured at the same time with canopy temperature.

Equation 4 represents a linear relationship between ET and the difference in temperature (*Tsc* – *Tac*). Using experimental field data on a wheat crop near Phoenix, Arizona, Jackson et al. (1977) concluded that the method could be used as a sound practical tool for determining crop water use requirements. The parameter *B* was determined to be 0.064 when (*ET* – *Rn*) was expressed in cm for the Phoenix experimental site. The major requirement for applications in other places was the need to re-calibrate the *B* parameter for new environmental conditions. Note that *Tsc* and *Tac* are comparable to *Ts* and *Tc* in equation 1, respectively.

In SPA, as opposed to equation 4, *Tc* is estimated as a function of the daily maximum air temperature over well-watered and well-vegetated surfaces using a *c* factor for calibration as shown in equation 5 (Senay et al., 2013, 2016, 2017).

$$Tc = c * T_{max} \quad (5)$$

where *c* is a factor that converts the daily maximum air temperature (T_{max}) into the equivalent of the wet/cold (*Tc*) reference surface temperature limit. Appendix A lists a set of equations in the estimation of *c* factor and other parameters of SSEBop.

While a weather station-based T_{max} can be used to represent a relatively large area in a uniform-hydro climatic region in equation 5, it is recommended to use gridded T_{max} for ET modeling over large and complex hydro-climatic regions where elevation, slope, and aspect can bring marked differences in air and surface temperatures within short distances. Although a single *c* factor can be used to provide a first order ET estimate using a seasonally averaged value for a given region (Senay et al., 2013), it could vary substantially by season and geographic region, requiring a dynamic *c* factor that needs to be calculated for each satellite image (Senay et al., 2017).

The dry-bulb (*Ts*) and wet-bulb (*Tc*) analogy in equation 1 requires at least two measurements in close proximity so that the evaporating cooling effect can be estimated as the difference between the *Ts* and *Tc*. Although this appears to be a challenging instrumentation problem, satellites record thermal responses of the landscape in a grid (raster), which is equivalent to several millions of thermometers to cover the globe. For example, one Landsat satellite, with 100 m spatial resolution (thermal) and a scene size of 170 km × 183 km, can be thought of as having about 3.1 million measurements of LST.

One of the critical challenges in SSEBop is the identification of wet-bulb equivalent surfaces in equation 5. In standard psychrometry, the wet-bulb is created by wrapping the bulb of one of the thermometers with a saturated wick (Lourence and Pruitt, 1969). Following the hot and cold pixel approach from the Surface Energy Balance Algorithm for Land (SEBAL) model (Bastiaanssen et al., 1998), the temperature of the wet/cold surface can be determined from a satellite image. In this case, the cold/wet limit is estimated using a combination of vegetation index and air temperature with the assumption that the rate of heating and evaporative cooling of the surface is in equilibrium and thus providing maximum ET, with little or no outgoing sensible heat from the surface, i.e., complete conversion of net radiation into latent heat flux at the wet/cold surface.

Finding well-distributed wet surfaces in close proximity to dry surfaces (any pixel) throughout a large satellite image is difficult and/or impossible in some cases. Note that all measurements of a satellite pixel can be thought of as ambient and thus represent the dry-bulb equivalent, but only a few locations (pixels) qualify for wet/cold reference. But, due to the stable and strong relationship between air temperature and satellite-based LST at the wet surface, the approach outlined in Senay et al. (2013, 2017) can be used to estimate the wet-bulb equivalent surface temperatures everywhere from gridded air temperature datasets (eq. 5).

The SSEBop formulation for establishing the wet/cold reference limit relies on the following assumptions: (1) the ambient air temperature measured by weather stations or spatially gridded data sources is representative of the air

temperature at the canopy level, (2) the canopy air temperature (meteorological) and canopy surface temperature (satellite measurement) are comparable and considered equal to the surface temperature at a well-watered, healthy vegetation (*Ts* = *Tc*). This is similar to the assumption by Bastiaanssen et al. (1998) where ET is considered maximum and sensible heat can be assumed to be zero at the wet/cold surface. In effect, this is the result of a surface energy balance at the canopy surface where the net radiation (less ground flux) is returned in a form of latent heat flux, providing evaporative cooling at the canopy surface.

While the idea of using air temperature as the wet/cold reference surface temperature is attractive, there are two main challenges that need to be overcome: (1) finding instantaneous air temperature data at the time of satellite overpass for operational applications over large areas is difficult, if not impossible, and (2) the air temperature and satellite surface temperature data are acquired and processed independently and are not expected to equate in absolute magnitude at the wet/cold reference location. However, daily maximum air temperature data are more readily available as compared to instantaneous or hourly time scales, which can be used to solve the first challenge. Secondly, because of the acquisition time and sensor type differences between satellite LST and air temperature measurements, the calibration coefficient (*c* factor) is applied to convert daily maximum air temperature into wet/cold (*Tc*) equivalent surface temperature as shown in equation 5 (Appendix A for details).

Psychrometric Constants: Air vs. Surface

Comparing the two psychrometric constants in equations 1 and 2, we may observe the similarities and differences between the two: the standard psychrometric constant is expressed in equation 6 by Allen et al. (1998). The constant value of 0.000665 was determined from empirical observations as early as 1886 as reported in Ferrel (1886) with a comparable formulation for actual vapor pressure determination.

$$\gamma = \frac{CpP}{\varepsilon\lambda} = 0.665 * 10^{-3} P \tag{6}$$

where *Cp* is specific heat of air at constant pressure, 1.013 10^{-3} (MJ.kg^{-1} °C^{-1}); *P* is atmospheric pressure (kPa); ε is ratio of molecular weight of water vapor to dry air, 0.622; and λ is latent heat of vaporization, 2.45 (MJ.kg^{-1}).

Although Lourence and Pruitt (1969) reported the dependence of γ on several factors such as air flow rate, radiation, air temperature, and others, the most common formulation simplifies to equation 6, which is mainly dependent on location (specifically, elevation) and expressed as a function of the local atmospheric pressure.

The surface psychrometric constant (γ^s) is formulated as below:

$$\gamma^s = \frac{C_p \rho}{Rn.r_{ah}} \tag{7}$$

where γ^s is a surface psychrometric constant (°C^{-1} or K^{-1}); *Cp* as defined in equation 6; ρ density of air (kg.m^{-3}); *Rn* daily average net radiation (MJ.m^{-2}.d^{-1}), f (location, day-of-year); r_{ah} aerodynamic resistance over bare soil, taken as 110 s.m^{-1} (Senay et al., 2013).

Unlike γ, the surface psychrometric constant (γ^s) (eq. 7) is also a function of day-of-year (DOY) in addition to location as it is mainly driven by net solar radiation. This is basically a reciprocal of the "*dT*" parameter in the original formulation of the SSEBop model (Senay et al., 2013). As the γ is the property of the dry air (Lourence and Pruitt, 1969), γ^s is also a property of a dry bare soil, i.e., the aerodynamic resistance for heat flow is calculated for an imaginary dry-bare soil (ET = 0) to estimate the maximum temperature difference between the bare surface and the canopy-level air temperature when all net radiation is converted into sensible heat (Senay et al., 2013). This formulation for *dT* or its inverse γ^s is interestingly comparable to the one put forward by Jackson et al. (1981) that is used to determine the maximum difference between canopy and air temperatures, which is obtained by setting the canopy resistance to infinity (non-transpiring surface).

The temporal evolution of γ^s (in a form of *dT*) for a point location (32.438° N, 109.956° W) within the study site (fig. 1) is shown in figure 2; *dT* is used to determine the hot/dry limit (*Th*) once the wet/cold limit is determined in equation 8 by simply adding *dT* to *Tc*.

$$Th = Tc + dT \tag{8}$$

where *Th* is the hot/dry reference limit (K); *Tc* the cold/wet reference temperature (K) as defined earlier; and *dT* (K) is simply the pre-defined temperature difference, calculated as the reciprocal of γ^s in equation 7.

Because γ^s is a constant, location- and day-specific values are pre-determined for every km^2 around the globe (Appendix A). This procedure eliminates the need to determine the hot/dry pixel reference limit, which is a requirement in the original formulation of ET fraction in the SSEB model (Senay et al., 2007). Note that equations shown in Appendix A are based on "average-sky" conditions as opposed to clear-sky conditions (Senay et al., 2013) for the calculation of daily average net radiation, which is a more reliable approximation of the daily radiation balance for days that acquire a successful satellite overpass (Appendix A for details).

From ET Fraction to Actual ET

While *ETf* using the SPA approach of SSEBop accounts for the limitations of ET, the estimation of actual ET (*ETa*) requires the determination of the maximum atmospheric demand. Although there are various methods to estimate atmospheric demand, the standardized Penman-Monteith (Allen et al., 1998) equation is widely used. Thus, equation 9 shows the *ETa* calculation using SPA formulation as a product of ET fraction (eq. 1) and atmospheric demand (reference ET) as shown below.

$$ETa = ETo - \gamma^s \left(Ts - Tc\right) ETo \tag{9}$$

where *ETa* is actual ET (mm); *ETo* is reference (maximum) ET (mm) – it is important to note that because *ETo* is based on the grass reference type, it may need an upscaling parameter "K" to simulate an aerodynamically rougher crop such

as alfalfa, whose value can be determined through a calibration process (Senay et al., 2013). A generally recommended value for "K" may lie between 1.2 and 1.3 (Allen et al., 1998, 2007); *Ts*, *Tc,* and γ^S are defined earlier.

The following set of equations show the derivation of the original SSEBop (Senay et al., 2007, 2013) from equation 9, indicating the comparability between SPA-based and original SSEBop expressions.

By substituting γ^S with $1/dT$, and factoring *ETo*, equation 9 can be written as:

$$ETa = \left(1 - \frac{Ts - Tc}{dT}\right) * ETo \quad (10)$$

By regrouping equation 10, ET fraction can be expressed as:

$$ETa = \frac{(Tc + dT) - Ts}{dT} * ETo \quad (11)$$

By simply substituting *Th* for *Tc* + *dT* (eq. 8), the following equation is the same as the original SSEBop formulation:

$$ETa = \frac{Th - Ts}{dT} * ETo \quad (12)$$

where *Th* is hot/dry reference surface temperature limit, which is now calculated as the sum of *Tc* and *dT,* eliminating the need to determine *Th* from the image. Other parameters are as defined earlier.

Thus, the derivation of equation 12 (original formulation) from equation 9 (SPA-based) shows "satellite psychrometric" formulation can provide a sound physical basis to explain the principles and working mechanisms of the SSEBop model.

Results

Illustrative Application

The SPA formulation is illustrated on an arbitrary transect over the Willcox Irrigation Basin in southern Arizona, figure 1 (Points A to B). The study area exhibits elevation ranges of more than 1,000 m varying from about 1,500 m to over 2,500 m. LST (*Ts*, K) was derived from Landsat 8 thermal imagery for the overpass date of 23 June 2014. Corresponding weather datasets were obtained from gridded data sources: daily maximum air temperature (*Tmax*) was obtained from the TopoWx dataset, which is available at 30 arc-second (~800 m) spatial resolution for the conterminous United States since 1948 (Oyler et al., 2015). For reference evapotranspiration, the gridded (4 km) daily grass reference evapotranspiration (*ETo*) dataset from (Abatzoglou, 2013) was used.

Figure 2 shows the temporal evolution of *dT* ($1/\gamma^S$) for a point ("C") location in the middle of the study site. It is important to note that *dT* is one of the two key variables of SSEBop (along with *Tc*) and can be calculated as the inverse of the surface psychrometric constant γ^S (eq. 7).

The importance and dominance of the net radiation in equation 7 is obvious in the temporal evolution of *dT,* which

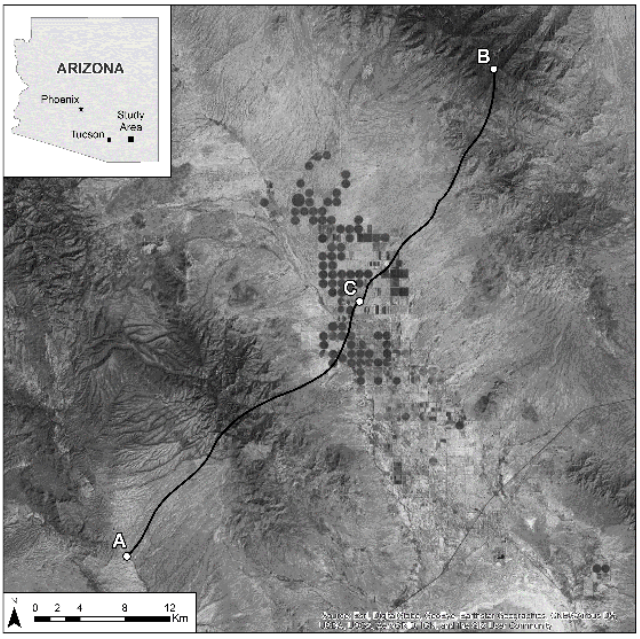

Figure 1. Location of Transect (A-B) in the Willcox Irrigation Basin, Arizona, southwestern United States. The irrigated area (shown by center pivots) is flanked by two mountains and surrounded by a dry landscape. Point C identifies the location for the time series chart shown in figure 2. The shape file and background imagery were downloaded from the ArcGIS open online database (https://www.arcgis.com/home/item.html?id=f7f805eb65eb4ab787a0a3e1116ca7e5).

reflects the seasonality of net radiation for the study location (fig. 1). Also, figure 2 shows low values in the winter (around 5K) and high values in the summer at around 23K, which coincides with the same high value for 23 June 2014, used in this example. Such $1/\gamma^S$ values are pre-determined for every 1 km^2 around the world under average-sky conditions (Appendix A); thus, eliminating the need to solve this constant during every satellite overpass. The addition of this constant to the lower cold/wet limit (*Tc*) will establish the upper hot/dry limit (*Th*) as shown in figure 3. Thus, *dT* ($1/\gamma^S$) eliminates the need to identify *Th* from the image.

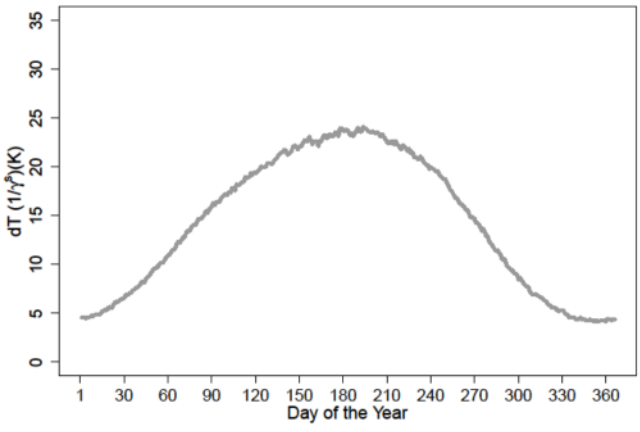

Figure 2. Temporal evolution of *dT* ($1/\gamma^S$) for point "C" at the study site (32.438° N, 109.956° W) for any given year, which is a solution for equation 7. The relatively smooth curve is a result of using climatological (average) conditions in the calculation of the daily average net radiation (Appendix A).

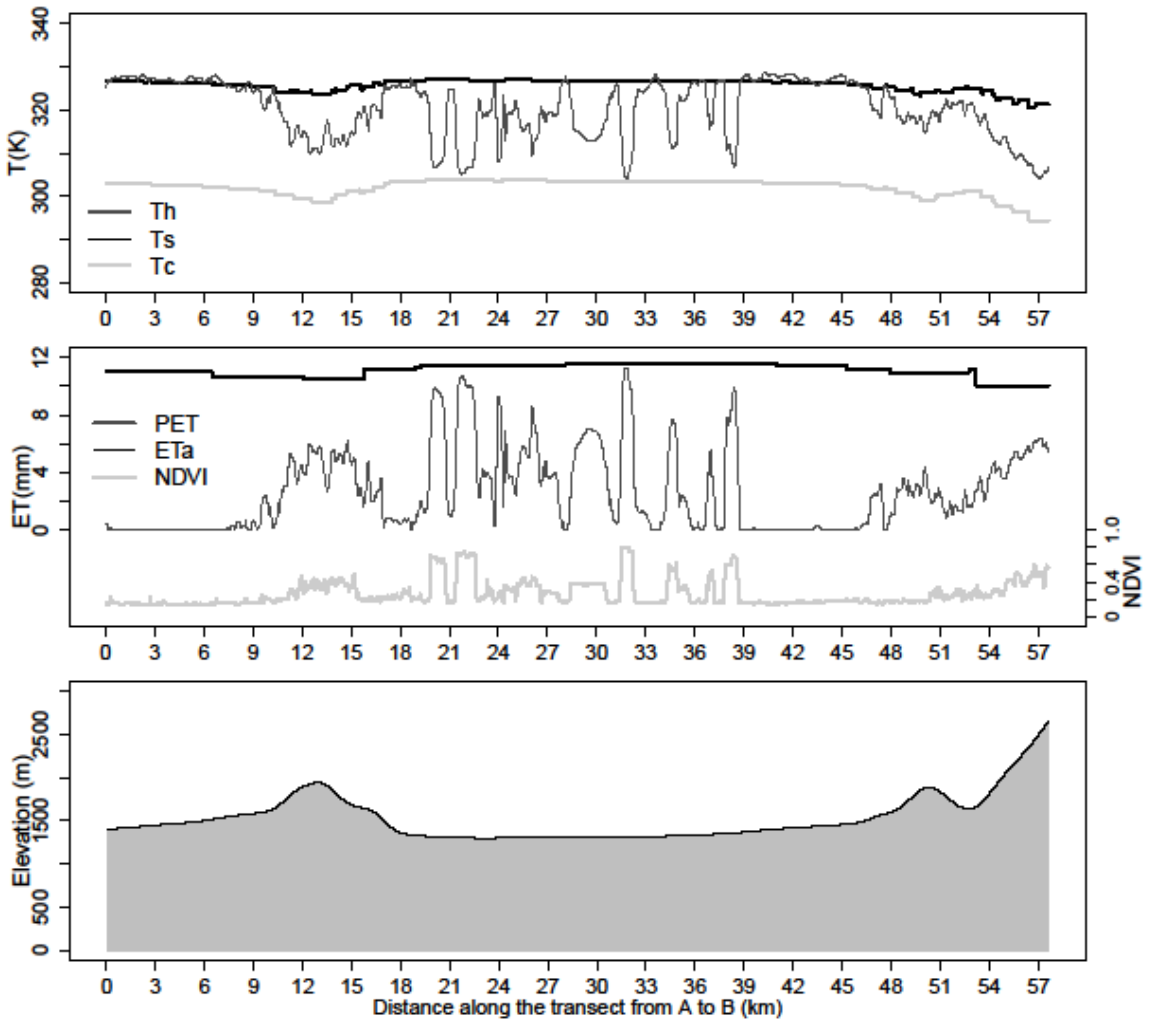

Figure 3. Top: Spatial patterns of *Ts*, *Tc* and *Th* along the study transect (A-B) in figure 1 for 23 June 2014. A c factor of 0.983 was used to convert *Tmax* to *Tc*. Middle: Spatial patterns of corresponding actual ET (*ETa*), up-scaled grass reference ET (PET for potential ET) and NDVI (Normalized Difference Vegetation Index). The NDVI (30 m spatial resolution) is included for a visual qualitative inspection on the spatial patterns of *ETa*. Bottom: elevation profile along the transect (A-B).

Figure 3 shows the relationships among hot/dry limit (*Th*), observed (*Ts)*, and cold/wet limit (*Tc*) for 23 June 2014, along transect A-B shown in figure 1. *Tc* is derived from the TopoWx daily maximum air temperature for the day using a *c* factor of 0.983, which was derived using equations 5. The lower panel shows the elevation profile of transect A-B. It is evident that *Tc* and *Ts* have different spatial characteristics; *Tc* varies slowly with marked changes appearing only with major elevation changes, making it more of a "regional" variable. On the other hand, *Ts* is more of a "local" variable with a high degree of variability in short distances. For example, in the middle of the valley (a section of up to 25 km) where there are center pivot irrigated fields, *Tc* varies little (<2K) whereas *Ts* can vary as much as 25K (fig. 3).

The relationships among the model-estimated actual ET (*ETa*), potential ET (PET: grass *ETo* that is scaled to alfalfa reference using a 1.25 factor) and NDVI for the same transect are shown in figure 3 (middle panel). As was the case with *Tc* and *Ts*, the reference ET (a regional variable) varies with little local dynamics (range between 9 and 11 mm), but *ETa* shows large variability (between 0 and 11 mm), making it a local variable. This reinforces the importance of *Ts* on actual ET estimation. But it is also important to note the crucial role of PET as it controls the seasonality of actual ET and its spatial dynamics at a regional scale. Although it was not possible to obtain independent validation datasets that represent the transect, which covers more than 50 km, the strong correspondence between NDVI and *ETa* patterns provides a qualitative check on the reasonableness of the SPA explanation of the SSEBop model. The performance of the SSEBop model against eddy covariance flux tower and other datasets have been published elsewhere (Velpuri et al., 2013; Singh et al., 2014; Singh and Senay, 2015; Chen et al., 2016; Senay et al., 2016, 2017). This is only an illustrative presentation to demonstrate the SPA formulation of SSEBop approach.

Figure 4 shows how the method can capture ET dynamics in a complex terrain that includes deserts, irrigated areas, and mountain vegetation. The contrasting ET values range from

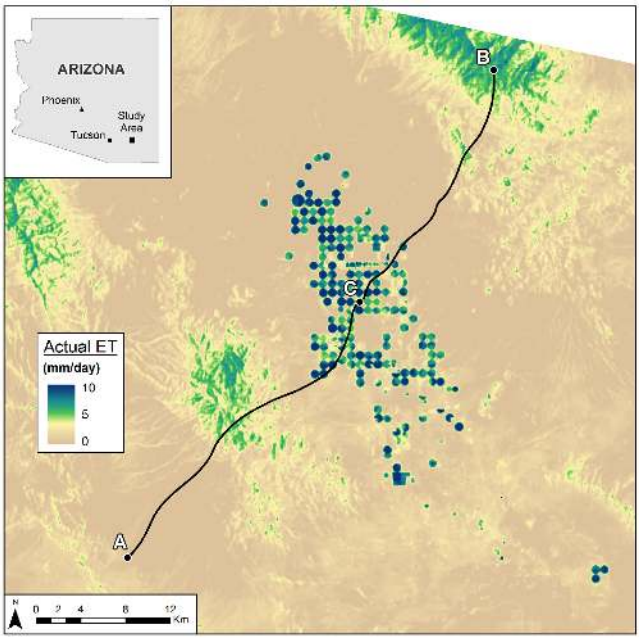

Figure 4. Actual ET map (23 June 2014) showing the relative distribution of Landsat-based ET across different landscapes that includes transect A-B shown in figure 3. The irrigated center pivots can be recognized as circular features. The map reveals differences in ET even within a single center pivot, which could come from differences in crop type and/or stage of the crop growth.

0 mm in the desert to maximum ET values of 11 mm in well irrigated center pivots and moderate ET values around 5 mm in the forested hills. This again demonstrates the robustness of a simple parameterization that can handle the complexity of the landscape using physically derived parameters from each pixel in the form of the air temperature for the cold/wet limit, the surface psychrometric constant γ^S ($1/dT$), and of course *Ts* and *ETo,* which are also gridded datasets.

DISCUSSION

As the SSEBop model uses important surface energy balance principles to determine model parameters such as the *dT* (the inverse of the newly coined "surface psychrometric constant, γ^S), the concern for not solving the full energy balance components should not invalidate the use of the phrase "simplified energy balance" in the model name. But, the new SPA formulation can be useful for understanding the physical basis of the model in a more familiar and established principle of psychrometry and encourages users to adapt and experiment with the model setup to estimate ET in diverse hydro-climatic systems.

As demonstrated, the SPA-formulation of SSEBop is comparable to the semi-empirical ET equation proposed by Jackson et al. (1977) as shown in equation 4. The most important difference is the use of a statistically derived "B" parameter in their formulation and the use of γ^S in SPA. Unlike the "B" parameter, γ^S is physically derived for each location from theoretical surface net radiation calculations and does not require calibration using locally measured temperature and flux datasets (ET, *Rn*). Interestingly, the "B" value, which was determined to be 0.064 (Jackson et al., 1981) for Phoenix, Arizona, is comparable to the seasonal average value of $\gamma^S = 0.069$ for Maricopa, Arizona, which is less than 75 km south of Phoenix. From figure 2, we can see the seasonal average *dT* value is about 14.4 K, whose inverse yields $\gamma^S = 0.069$. However, this close match between "B" and γ^S could be accidental as the "B" parameter is a statistical value that depends on the specific experimental setup including units of parameters; thus, no direct comparability is being suggested except the similarity in the form of the two equations.

The reasonable performance of the SSEBop model has been documented by several researchers. Of course, its performance, like any other model, depends on the input data quality and model parameterization. For example, Senay et al. (2013) reported that while validation against individual flux towers can vary greatly from explaining 70% to 97% of the observed variance, Velpuri et al. (2013) reported an overall basin scale accuracy of 75% for annual estimates in the United States. Chen et al. (2016) concluded that the overall uncertainty of the SSEBop model as a result of combined errors in model parameters and input variables is less than 20% when evaluated across 42 eddy covariance sites in diverse biomes in the United States at monthly time scales. Compared with other models, Singh and Senay (2015) found that SSEBop model performance was comparable to three other surface energy balance models, including SEBAL (Bastiaanssen, et al., 1998), Measuring Evapotranspiration at High Resolution with Internalized Calibration (METRIC) (Allen et al., 2007) and Surface Energy Balance System (SEBS) (Su, 2002). Similarly, Bezerra et al. (2015) compared SEBAL and SSEB in a cotton experimental field in Brazil using Landsat-5 images and found the performance of the two models to be comparable. Bhattarai et al. (2016) reported a lower performance for SSEBop when compared to ET estimates from four other surface energy balance models [SEBAL, SEBS, METRIC, Simplified Surface Energy Balance Index (S-SEBI)] in the humid southeastern United States.

Generally, performance of SSEBop/SPA depends on model parameterization and the quality of forcing input data. These include the focus on the two model parameters: cold/wet limit (*Tc)* and surface psychrometric constant γ^S ($1/dT$). For model inputs, obviously the quality of LST and the reference ET are the most important determinants. The following discussion lists important considerations for estimating ET over complex landscapes using the SPA-formulated SSEBop.

SSEBOP AS A TWO-PARAMETER MODEL

Equation 1 shows that the SPA formulation makes SSEBop a two-parameter model to estimate ET fraction: *Tc* and γ^S. Of the two parameters, *Tc* appears more critical as it determines the magnitude of the difference from the observed satellite *Ts* and hence the *ETf*. While γ^S is also an important parameter, it varies gradually in space and DOY and does not vary from year-to-year, thus introducing minimal randomness in the overall ET estimation. However, γ^S can introduce a substantial bias in the overall ET estimation. Therefore, SPA formulation of SSEBop stresses the im-

portance of evaluating and calibrating the *Tc* and γ^S parameters before implementing the model in the calculation of ET fraction and ET.

C Factor Calibration for Tc Estimation

Determining the c factor is a crucial step as it determines the accuracy of the Tc parameter for the wet/cold boundary condition (Senay et al., 2017). The method works well when there is enough dense vegetation with high NDVI (>0.70) values in a satellite image. The challenge is in regions and seasons where it is impossible to obtain well vegetated pixels with the threshold NDVI > 0.7. In these scenarios, it is best to use a median c factor from the available images in a year. Because c factor is generally stable throughout the year, with some seasonal dynamics in certain locations, and the median tends to come from the growing season, using this growing season median during the off season is a reasonable substitution. For Landsat, the c factor is estimated from the scene-wide image (170 km × 183 km). On the other hand, due to its large size, it is advisable to sub-divide a MODIS (MODerate Resolution Imaging Spectroradiometer) tile (10° × 10°) into smaller sections with each section representing about 200 km × 200 km.

Lapse Rate

In complex mountainous regions, the most important working assumption is that the environmental lapse rate for both air temperature (*Ta*) and LST (*Ts*) are comparable over sparsely vegetated dry surfaces (minimal evaporative cooling). From experience this does not seem to hold in high mountains especially for elevation greater than 2,500 m or isolated mountains in lower elevations. At times, the *Ts* appears to cool faster with elevation than the *Ta,* which will result in an overestimation of ET in such situations. More research is required to evaluate the impact of this differential lapse rate and implement a physically derived adjustment.

Challenges in Low ET Surfaces and Seasons

Although the absolute error is small, the relative ET error tends to be high when the surface is dry (water limiting) or too cold as in the case of the winter season (energy limited). The inverse of γ^S (*dT*) tends to vary from a low of 2 K to a high of 25 K or more. The low value is found during the winter season (cold climates) in higher or lower latitudes. With the accuracy of LST at about 1 K on vegetated surfaces and as high as 5 K on desert surfaces (Chen et al., 2016), it is best to keep the minimum *dT* at about 6 K. On the other hand, the maximum *dT* tends to be found in high mountains as a result of the lower density of air, which creates a larger separation between the surface and canopy temperature that the *dT* represents. A higher *dT* tends to give a higher ET fraction for the same *Tc* and *Ts,* which will overestimate the ET fractions in high mountains. Thus, because of the uncertainty in the *dT* calculation, it is best to limit the maximum *dT* at about 25 K. Similarly, users are encouraged to evaluate if *dT* = 25 K as the upper limit is reasonable for their study site. Furthermore, the accuracy of *Ts* tends to be lower in sparsely vegetated areas such as desert landscapes with complications from increased albedo in sands and changing emissivity values in darker parent material, sometimes resulting in a LST that appears much colder than expected, thereby overestimating ET. Thus, the application of this approach requires careful examination of the reasonableness of the input variable, *Ts*, so that model adjustment can be made on such surfaces. Although such uncertainty mainly affects the surfaces with low ET values, it will create unrealistic ET artifacts in such desert landscapes thereby casting doubt in the reliability of the method for vegetated landscapes where much of the intent and interest resides.

Cloud Filling and Seasonal Estimation

One of the challenges of optical and thermal remote sensing is haze, clouds and/or cloud contamination and their shadows. Generally, ET fractions in excess of 1.3 are found in clouded pixels and become masked values (no data) due to their unreliability from cloud or cloud shadow contamination. Thus, ET fractions in excess of 1.3 have to be filled by interpolation from adjacent periods, generally assuming linear relationships between two consecutive satellite dates. Similarly, monthly and seasonal ET are simply generated by summing the product of ET fractions and reference ET over the given aggregation period. Thus, the final seasonal product will depend on the availability of images and the accuracy of the interpolation technique to fill missing/masked image pixels.

Capping ET Fractions

For practical and meaningful applications, negative ET fractions are set to 0 and maximum *ETf* is limited to 1.05. The 5% additional "buffer" is to include those pixels that may experience a surface temperature that is colder than the estimated *Tc*, following a similar justification and recommendation by Senay et al. (2016). *ETf* can become unrealistically negative (*ETf* < 0) when *Ts* is higher than *Th* in arid and semi-arid locations, or too high (*ETf* > 1.0) in wet and cold landscapes when *Ts* is much lower than *Tc*. These are mainly a result of errors associated with *Tc* and γ^S estimations. While negative *ETf* values can be set to 0 with a reasonable justification, values greater than one (*ETf* > 1) are handled differently to avoid excluding valid pixels. Thus, in operational modeling, covering large areas, ET fractions between 1.05 and 1.3 are set to 1.05, but *ETf* that are greater than 1.3 are considered too cold and suspected of being contaminated by clouds and will be assigned to a no data value and thus have to be filled through temporal interpolation.

Although capping of ET fractions avoids unrealistic ET estimations, the overall ET estimation depends on the quality and accuracy of the model forcings (LST and ETo) in addition to the two model parameters (*Tc* and γ^S).

Validation of ET

Validation and calibration of the SSEBop ET estimates are necessary especially when the model is applied to a new region with unknown bias and random errors, which could come from a combination of model parameters and input variables. Depending on availability of the validation data and purpose of the ET maps, the validation techniques may range from daily total to monthly, seasonal and annual magnitudes. Model estimates tend to be more reliable at longer

aggregation periods due to the benefit of averaging on random errors while the bias persists at all scales (Senay et al., 2014a). In addition to daily measurements from eddy covariance flux towers (Baldocchi et al., 2001), Bowen ratio (Bowen, 1926) and lysimeters (Gowda et al., 2009; Allen et al., 2011), basin-scale water balance ET can be used to evaluate the performance of remote sensing ET at an annual time scale as a difference between basin-wide precipitation and discharge measurements, assuming negligible basin storage change (Velpuri et al., 2013; Bastiaanssen et al., 2014; Senay et al., 2014b).

The performance of the model can be improved by correcting for any bias that could be obtained from annual scale error analysis where the random component is minimal and the bias error dominate. It is important to note that the impact of weather variability on actual ET is handled through ETo and the impact of land cover is supposed to be handled by LST itself. Although the absolute accuracy of LST is not critical as the relative difference with the cold/wet limit is the driver (eq. 1), the absolute magnitude of ETo is crucial in determining the magnitude of actual ET.

CONCLUSION

The Satellite Psychrometric Approach (SPA) formulation of the SSEBop model is presented with the rearrangement of equations and redefining model parameters without any fundamental change in the SSEBop approach. For example, ET fraction is now calculated as the difference between *Ts* and *Tc* without the need for specifying the hot/dry reference limit. To complete the parallel with standard psychrometry for relative humidity estimation whose psychrometric constant varies only with location (as a function of atmospheric pressure), a new constant is defined as the surface psychrometric constant γ^S ($1/dT$), which varies only with location and day-of-year.

The SPA formulation may be considered an enhancement of the Jackson et al. (1977) ET equation in three aspects: (1) the use of daily maximum air temperature instead of using hourly air temperature directly for the cold/wet reference surface temperature (*Tc*); (2) the use of a physically derived spatio-temporally dynamic surface psychrometric constant (γ^S) instead of the "B" parameter, which is static over a season and requires observed datasets on new locations; and (3) the use of *ETo* instead of *Rn*, thanks to the increasing availability of regional and global gridded weather datasets.

It is believed that the SPA explanation strengthens the physical basis for SSEBop and shows the robustness of the method in diverse ecosystems since it uses physical parameters from each pixel whether it is gridded air temperature or γ^S and model drivers such as LST and gridded reference ET. With only two parameters, users can improve the performance of the model by calculating γ^S and *Tc* using more accurate datasets for localized applications instead of using coarse global datasets. With a one-time calibration for bias removal, the model is capable of processing historical remote sensing data going back to 1984 (Senay et al., 2017). Similarly, Alemayehu et al. (2017) demonstrated the effectiveness of the two-parameter formulation for ET mapping in the Mara Basin, a hydro-climatically complex system in East Africa.

While using the SPA formulation of SSEBop reinforces parameter simplification, the model continues to be an effective method for reliable estimation and explanation of satellite-based ET for several applications in agriculture and hydrology. Because of the consistency of the model output, SSEBop products are useful not only for drought monitoring purposes where relative changes are important, but also for more robust water use assessments at local and global scales.

ACKNOWLEDGEMENT

This research work was supported by the U.S. Geological Survey (USGS) Land Change Science (LCS) Program in support of water use and water budget studies in the United States and international applications. Special thanks go to MacKenzie Friedrichs and Manohar Velpuri for creating the graphics along with Matthew Schauer. The continued development and implementation of SSEBop for large-scale monitoring of landscape water use has been possible with the continued effort of Stefanie Kagone. Ramesh Singh and Manohar Velpuri have contributed to the continued recognition of the model through comprehensive evaluation procedures using varied data sources from flux towers to water balance approaches. Great appreciation is extended to Dr. Prasanna Gowda and two other anonymous reviewers for their constructive and insightful comments. The USGS Earth Resources and Observation Science Center deserves credit for creating a conducive research environment to develop, advance and implement remote sensing-based techniques for large-scale terrestrial monitoring. Any use of trade, firm, or product names is for descriptive purposes only and does not imply endorsement by the U.S. Government. Data used in support of this study are available in Senay (2018).

REFERENCES

Abatzoglou, J. T. (2013). Development of gridded surface meteorological data for ecological applications and modelling. *Int. J. Climatol., 33*(1), 121-131. https://doi.org/10.1002/joc.3413

Alemayehu, T., van Griensven, A., Senay, G. B., & Bauwens, W. (2017). Evapotranspiration mapping in a heterogeneous landscape using remote sensing and global weather datasets: Application to the Mara Basin, East Africa. *Remote Sensing, 9*(4), 390. https://doi.org/10.3390/rs9040390.

Allen, R. G., Pereira, L. S., Howell, T. A., & Jensen, M. E. (2011). Evapotranspiration information reporting: I. Factors governing measurement accuracy. *Agric. Water Manag., 98*(6), 899-920. https://doi.org/10.1016/j.agwat.2010.12.015

Allen, R. G., Pereira, L. S., Raes, D., & Smith, M. (1998). Crop evapotranspiration: Guidelines for computing crop water requirements. *FAO Irrigation and Drainage Paper* (Vol. 56). Rome: FAO.

Allen, R. G., Tasumi, M., Morse, A., Trezza, R., Wright, J. L., Bastiaanssen, W., ... Robison Clarence, W. (2007). Satellite-based energy balance for mapping evapotranspiration with internalized calibration (METRIC)-applications. *J. Irrig. Drain. Eng., 133*(4), 395-406. https://doi.org/10.1061/(ASCE)0733-9437(2007)133:4(395)

Anderson, M. C., Norman, J. M., Diak, G. R., Kustas, W. P., and Mecikalski, J. R. 1997. A two-source time-integrated model for estimating surface fluxes using thermal infrared remote sensing. *Remote Sensing Environment 60*(2), 195-216. https://doi.org/10.1016/S0034-4257(96)00215-5

Baldocchi, D., Falge, E., Gu, L., Olson, R., Hollinger, D., Running, S., ... Wofsy, S. (2001). FLUXNET: A new tool to study the temporal and spatial variability of ecosystem-scale carbon dioxide, water vapor, and energy flux densities. *Bull. American Meteorological Soc., 82*(11), 2415-2434. https://doi.org/10.1175/1520-0477(2001)082<2415:fantts>2.3.co;2

Bastiaanssen, W. G., Menenti, M., Feddes, R. A., & Holtslag, A. A. (1998). A remote sensing surface energy balance algorithm for land (SEBAL). 1. Formulation. *J. Hydrol., 212-213*, 198-212. https://doi.org/10.1016/S0022-1694(98)00253-4

Bastiaanssen, W., Karimi, P., Rebelo, L.-M., Duan, Z., Senay, G., Muthuwatte, L., & Smakhtin, V. (2014). Earth observation based assessment of the water production and water consumption of nile basin agro-ecosystems. *Remote Sensing, 6*(11), 10306-10334. https://doi.org/10.3390/rs61110306

Bezerra, B. G., Silva, B. B., Santos, C. A., & Bezerra, J. R. (2015). Actual evapotranspiration estimation using remote sensing: comparison of SEBAL and SSEB approaches. *Adv. Remote Sensing, 4*(3), 234-247. https://doi.org/10.4236/ars.2015.43019

Bhattarai, N., Shaw, S. B., Quackenbush, L. J., Im, J., & Niraula, R. (2016). Evaluating five remote sensing based single-source surface energy balance models for estimating daily evapotranspiration in a humid subtropical climate. *Int. J. Appl. Earth Observation Geoinformation, 49*, 75-86. https://doi.org/10.1016/j.jag.2016.01.010

Bowen, I. S. (1926). The ratio of heat losses by conduction and by evaporation from any water surface. *Physical Rev., 27*(6), 779-787. Retrieved from https://link.aps.org/doi/10.1103/PhysRev.27.779

Campbell, G. S. (1979). Improved thermocouple psychrometers for measurement of soil water potential in a temperature gradient. *J. Physics E: Scientific Instruments, 12*, 1-5. https://doi.org/10.1088/0022-3735/12/8/018

Carlson, T. (2007). An overview of the "triangle method" for estimating surface evapotranspiration and soil moisture from satellite imagery. *Sensors, 7*(8), 1612. https://doi.org/10.3390/s7081612

Chen, M.S., Senay, G.B., Singh, R.K., & Verdin, J. P. (2016). Uncertainty analysis of the Operational Simplified Surface Energy Balance (SSEBop) model at multiple flux tower sites. *Journal of Hydrology, 536*, 384-399. doi: 10.1016/j.jhydrol.2016.02.026.

Ferrel, W. M. (1886). Annual Report. 223-259. Chief U.S. Signal Office.

Fisher, J. B., DeBiase, T. A., Qi, Y., Xu, M., & Goldstein, A. H. (2005). Evapotranspiration models compared on a Sierra Nevada forest ecosystem. *Environ. Model. Software, 20*(6), 783-796. https://doi.org/10.1016/j.envsoft.2004.04.009

Fuchs, M., & Tanner, C. B. (1970). Error analysis of bowen ratios measured by differential psychrometry. *Agric. Meteorol., 7*, 329-334. https://doi.org/10.1016/0002-1571(70)90027-0

Glenn, E. P., Huete, A. R., Nagler, P. L., Hirschboeck, K. K., & Brown, P. (2007). Integrating remote sensing and ground methods to estimate evapotranspiration. *Critical Rev. Plant Sci., 26*(3), 139-168. https://doi.org/10.1080/07352680701402503

Gowda, P. H., Senay, G. B., Howell, T. A., & Marek, T. H. (2009). Lysimetric evaluation of simplified surface energy balance approach in the Texas High Plains. *Appl. Eng. Agric., 25*(5), 665-669. https://doi.org/10.13031/2013.28855

Jackson, R. D., Idso, S. B., Reginato, R. J., & Pinter, P. J. (1981). Canopy temperature as a crop water stress indicator. *Water Resour. Res., 17*(4), 1133-1138. https://doi.org/10.1029/WR017i004p01133

Jackson, R. D., Reginato, R. J., & Idso, S. B. (1977). Wheat canopy temperature: A practical tool for evaluating water requirements. *Water Resour. Res., 13*(3), 651-656. https://doi.org/10.1029/WR013i003p00651

Kustas, W. P., & Norman, J. M. (2000). A two-source energy balance approach using directional radiometric temperature observations for sparse canopy covered surfaces. *Agron. J., 92*(5), 847-854. https://doi.org/10.2134/agronj2000.925847x

Liddell, H. G., & Scott, R. (1940). *A Greek-English Lexicon. revised and augmented throughout by Sir Henry Stuart Jones with the assistance of Roderick McKenzie.* Oxford: Clarendon Press.

Lourence, F. J., & Pruitt, W. O. (1969). A psychrometer system for micrometeorology profile determination. *J. Appl. Meteorol., 8*(4), 492-498. https://doi.org/10.1175/1520-0450(1969)008<0492:apsfmp>2.0.co;2

Moran, M. S., Rahman, A. F., Washburne, J. C., Goodrich, D. C., Weltz, M. A., & Kustas, W. P. (1996). Combining the Penman-Monteith equation with measurements of surface temperature and reflectance to estimate evaporation rates of semiarid grassland. *Agric. For. Meteorol., 80*(2), 87-109. https://doi.org/10.1016/0168-1923(95)02292-9

Mu, Q., Zhao, M., & Running, S. W. (2011). Improvements to a MODIS global terrestrial evapotranspiration algorithm. *Remote Sensing Environ., 115*(8), 1781-1800. https://doi.org/10.1016/j.rse.2011.02.019

Nagler, P. L., Cleverly, J., Glenn, E., Lampkin, D., Huete, A., & Wan, Z. (2005). Predicting riparian evapotranspiration from MODIS vegetation indices and meteorological data. *Remote Sensing Environ., 94*(1), 17-30. https://doi.org/10.1016/j.rse.2004.08.009

Oyler, J. W., Ballantyne, A., Jencso, K., Sweet, M., & Running, S. W. (2015). Creating a topoclimatic daily air temperature dataset for the conterminous United States using homogenized station data and remotely sensed land skin temperature. *Int. J. Climatol., 35*(9), 2258-2279. 10.1002/joc.4127

Penman, H. L. (1948). Natural evaporation from open water, bare soil and grass. *Proc. of the Royal Society of London. Series A. Mathematical Physical Sci., 193*(1032), 120-146. https://doi.org/10.1098/rspa.1948.0037

Penman, H. L. (1955). Humidity. *Q. J. Royal Meteorological Soc., 82*(352), 252-253.

Rawlins, S. L. (1966). Theory for thermocouple psychrometers used to measure water potential in soil and plant samples. *Agric. Meteorol., 3*(5), 293-310. https://doi.org/10.1016/0002-1571(66)90013-6

Roerink, G. J., Su, Z., & Menenti, M. (2000). S-SEBI: A simple remote sensing algorithm to estimate the surface energy balance. *Phys. Chem. Earth Part B, 25*(2), 147-157. https://doi.org/10.1016/S1464-1909(99)00128-8

Senay, G. B. (2018). Landsat-based illustrative implementation of Satellite Psychrometry for ET Mapping. *U.S. Geological Survey data release.* doi.org/10.5066/F7ZS2VR6

Senay, G., Budde, M., Verdin, J., & Melesse, A. (2007). A coupled remote sensing and simplified surface energy balance approach to estimate actual evapotranspiration from irrigated fields. *Sensors, 7*(6), 979. https://doi.org/10.3390/s7060979

Senay, G. B., Bohms, S., Singh, R. K., Gowda, P. H., Velpuri, N. M., Alemu, H., & Verdin, J. P. (2013). Operational evapotranspiration mapping using remote sensing and weather datasets: A new parameterization for the SSEB approach. *JAWRA, 49*(3), 577-591. https://doi.org/10.1111/jawr.12057

Senay, G. B., Gowda, P. H., Bohms, S., Howell, T. A., Friedrichs, M., Marek, T. H., & Verdin, J. P. (2014a). Evaluating the SSEBop approach for evapotranspiration mapping with landsat data using lysimetric observations in the semi-arid Texas High Plains. *Hydrol. Earth Syst. Sci. Discuss., 11*, 723-756. https://doi.org/10.5194/hessd-11-723-2014

Senay, G. B., Leake, S., Nagler, P. L., Artan, G., Dickinson, J., Cordova, J. T., & Glenn, E. P. (2011). Estimating basin scale evapotranspiration (ET) by water balance and remote sensing methods. *Hydrol. Processes, 25*, 4037-4049. https://doi.org/10.1002/hyp.8379

Senay, G. B., Velpuri, N. M., Bohms, S., Demissie, Y., & Gebremichael, M. (2014b). Understanding the hydrologic sources and sinks in the Nile Basin using multisource climate and remote sensing data sets. *Water Resour. Res., 50*(11), 8625-8650. https://doi.org/10.1002/2013WR015231

Senay, G. B., Friedrichs, M., Singh, R. K., & Velpuri, N. M. (2016). Evaluating Landsat 8 evapotranspiration for water use mapping in the Colorado River Basin. *Remote Sensing Environ., 185*, 171-185. https://doi.org/10.1016/j.rse.2015.12.043

Senay, G. B., Schauer, M., Friedrichs, M., Velpuri, N. M., & Singh, R. K. (2017). Satellite-based water use dynamics using historical Landsat data (1984-2014) in the southwestern United States. *Remote Sens. Environ., 202*, 98-112. https://doi.org/10.1016/j.rse.2017.05.005

Singh, R., & Senay, G. (2015). Comparison of four different energy balance models for estimating evapotranspiration in the midwestern United States. *Water, 8*(1), 9. https://doi.org/10.3390/w8010009

Singh, R., Senay, G., Velpuri, N., Bohms, S., Scott, R., & Verdin, J. (2014). Actual evapotranspiration (water use) assessment of the Colorado River Basin at the landsat resolution using the operational simplified surface energy balance model. *Remote Sensing, 6*(1), 233. https://doi.org/10.3390/rs6010233

Slatyer, R. O., & Bierhuizen, J. F. (1964). A differential psychrometer for continuous measurements of transpiration. *Plant Physiol., 39*(6), 1051-1056. https://doi.org/10.1104/pp.39.6.1051

Su, Z. (2002). The Surface Energy Balance System (SEBS) for estimation of turbulent heat fluxes. *Hydrol. Earth Syst. Sci., 6*(1), 85-100. https://doi.org/10.5194/hess-6-85-2002

Velpuri, N. M., Senay, G. B., Singh, R. K., Bohms, S., & Verdin, J. P. (2013). A comprehensive evaluation of two MODIS evapotranspiration products over the conterminous United States: Using point and gridded FLUXNET and water balance ET. *Remote Sensing Environ., 139*, 35-49. https://doi.org/10.1016/j.rse.2013.07.013

APPENDIX A

SSEBop with SPA Formulation (A.1-A.5). Detailed explanation for A.6 to A.14 is found in Allen et al. (1998).

$$ETa = ETf * K * ETo \tag{A.1}$$

$$ETf = 1 - \frac{Ts - Tc}{dT} \tag{A.2}$$

$$Tc = c * T_{max} \tag{A.3}$$

$$c = \frac{Ts\_cold}{T_{max}} \tag{A.4}$$

$$dT = \frac{Rn * r_{ah}}{\rho_a * C_p} \tag{A.5}$$

$$Rn = Rns - Rnl \tag{A.6}$$

$$Rns = (1 - \alpha) * Rs \tag{A.7}$$

$$Rs = k_{Rs} \sqrt{(T_{max} - T_{min})} * R_a \tag{A.8}$$

$$Rso = (0.75 + 2 * 10^{-5} * Z) * Ra \tag{A.9}$$

$$Rnl = \sigma \left(\frac{T_{max}^4 + T_{min}^4}{2} \right) * \left(0.34 - 0.14\sqrt{ea}\right) \left(1.35 * \frac{Rs}{Rso} - 0.35\right) \tag{A.10}$$

$$\rho_a = \frac{1000 * P}{T_{kv} * R} = 3.486 * \frac{P}{T_{kv}} \tag{A.11}$$

$$P = 101.3 \left(\frac{293 - 0.0065 * Z}{293} \right)^{5.26} \tag{A.12}$$

$$T_{kv} = 1.01 \left(\frac{T_{max} + T_{min}}{2} + 273.15 \right) \tag{A.13}$$

$$ea = e^{\left(\frac{17.27 * T_{min}}{T_{min} * 237.3}\right)} \tag{A.14}$$

where

ETa = actual ET (mm)
ETo = grass reference ET (mm)
ETf = ET fraction (-)
K = maximum ET scaling factor (grass to alfalfa conversion, average at 1.2) (-)
Tc = cold/wet reference limit for surface temperature (K)
Ts_cold = land surface temperature from well-vegetated surfaces (K)
Tmin, *Tmax* = minimum and maximum air temperature (K)
dT(1/γ^S) = temperature difference between hot/dry ground and cold/wet canopy reference points (K)
c = factor converting air temperature into cold surface temperature (-)
Rn = net radiation (MJ.m^{-2}.d^{-1})
Rns = net shortwave radiation (MJ.m^{-2}.d^{-1})
Rnl = net long wave radiation (MJ.m^{-2}.d^{-1})
Rs = incoming solar radiation (average-sky) (MJ.m^{-2}.d^{-1})
Rso = incoming clear-sky radiation (MJ.m^{-2}.d^{-1})
Ra = extraterrestrial solar radiation (MJ.m^{-2}.d^{-1})
α = albedo, fraction of reflected incoming shortwave radiation on bare ground (~0.23^{+})
σ = Stefan-Boltzmann constant (4.903*10^{-9} MJ.K^{-4}.m^{-2}.d^{-1})
r_{ah} = aerodynamic resistance to heat transfer (~110^{+} s.m^{-1})
ρ_a = air density (Kg.m^{-3})
P = atmospheric pressure (kPa)
Z = elevation (m)

T_{kv} = virtual air temperature (K), dry air must be heated to equal the density of moist air at the same pressure.
C_p = specific heat of air (1.013 $kJ.Kg^{-1}C^{-1}$)
k_{Rs} = adjustment coefficient (0.16-0.19 $°C^{-0.5}$)
R = specific gas constant (287 $J.Kg^{-1}.K^{-1}$)
ea = actual vapor pressure (kPa)
$^{+}$ = these values are used to produce a calibrated dT using equations A.5 and A.7.

NOTES

1. The *c* factor is calculated from a ratio between *Ts_cold* and *Tmax* (eq. A.4) as a spatial average from several hundred to thousand pixels, representing wet surfaces (healthy vegetation) where the conditions for maximum ET are expected to be met. *Ts_cold* is the LST from well-watered and fully developed vegetated surfaces; it is only obtained from LST at calibration points, guided by NDVI whereas *Tc* is available for every pixel and is derived from *Tmax,* a climatology *Tmax* can be used. More detail is provided in Senay et al. (2017).
2. Equation A.8 is a new modification compared to the approach followed in Senay et al. (2013) where clear-sky was assumed. In this case, "average-sky" condition is used to estimate the incoming daily radiation which in turn is used in the calculation of short- and longwave radiation and eventually *dT*. The average-sky condition assumes a given pixel in a given day will be subjected to an average cloud cover for the rest of the day despite the clear-sky condition during the instantaneous moment of satellite overpass, avoiding a general overestimation of the net radiation which would lead to a higher *dT* and higher ET. It is important to note that actual net radiation data could be more accurate than average-sky condition; however, for the purpose of establishing the hot/dry boundary limit, the average-sky condition suffices for operational applications in addition to its advantage for computational simplicity.